processes

MDPI

Article

Evaluation of Adsorbent Biomaterials Based on Coconut Mesocarp for Treatment of Wastewater Contaminated with Tartrazine Dye

Candelaria Tejada-Tovar [1], Ángel Villabona-Ortiz [1], Fabián Aguilar-Bermúdez [1], Yerardin Pájaro-Moreno [1] and Ángel Darío González-Delgado [2,*]

[1] Process Design, and Biomass Utilization Research Group (IDAB), Chemical Engineering Department, Universidad de Cartagena, Avenida del Consulado St. 30, Cartagena de Indias 130015, Colombia; ctejadat@unicartagena.edu.co (C.T.-T.); avillabonao@unicartagena.edu.co (Á.V.-O.); faguilarb@unicartagena.edu.co (F.A.-B.); ypajarom@unicartagena.edu.co (Y.P.-M.)

[2] Chemical Engineering Department, Nanomaterials and Computer-Aided Process Engineering Research Group (NIPAC), Universidad de Cartagena, Avenida del Consulado St. 30, Cartagena de Indias 130015, Colombia

* Correspondence: agonzalezd1@unicartagena.edu.co

Abstract: The presence of synthetic dyes in industrial wastewater poses significant environmental and health concerns due to their persistent nature and potential toxicity. Tartrazine is a synthetic yellow dye known for its stability and resistance to conventional treatment methods. As a result, its discharge into natural water bodies can lead to adverse ecological impacts and can jeopardize public health. The objective of this work was to functionalize coconut shells (CSs), coconut cellulose (CC), and modified coconut cellulose (MCC) bioadsorbents with cetyl trimethyl ammonium chloride (CTAC) for their use in the elimination by adsorption of the dye tartrazine in aqueous solutions. CC was synthesized through a double extraction with sodium hydroxide, and a chemical treatment was performed with CTAC at 100 mmol L^{-1}. The final dye concentration was determined through UV-Vis at 500 nm. An FTIR analysis showed multiple active sites, represented in groups such as hydroxyl, COO-, NHx-, and hydrocarbon compounds. Increasing the initial concentration had a positive effect on the efficiency of the process, reaching 99% removal with an adsorption capacity of 11.89 mg/g at equilibrium using MCC. The test showed that equilibrium was reached after 30 min. Initially, the removal of the dyes was rapid, about 97% of the contaminant being removed in the first 5 min. The Langmuir and Freundlich models were satisfactorily fitted to the adsorption isotherm, showing physical and chemical adsorption. It can be concluded that MCC is a promising bioadsorbent for the removal of tartrazine dye in aqueous solutions.

Keywords: azo-anionic dye; bioadsorption; coconut waste; tartrazine; water treatment

Citation: Tejada-Tovar, C.; Villabona-Ortiz, Á.; Aguilar-Bermúdez, F.; Pájaro-Moreno, Y.; González-Delgado, Á.D. Evaluation of Adsorbent Biomaterials Based on Coconut Mesocarp for Treatment of Wastewater Contaminated with Tartrazine Dye. *Processes* **2023**, *11*, 3115. https://doi.org/10.3390/pr11113115

Academic Editors: José Cleiton Sousa dos Santos and Maria Alexsandra De Sousa Rios

Received: 26 July 2023
Revised: 12 September 2023
Accepted: 12 September 2023
Published: 31 October 2023

1. Introduction

Over time, renewable materials have been used to create ecofriendly products, making green supply chains a widely used method for improving ecosystems, improving the environment, and reducing energy consumption, among others [1]. Many paper, pulp, food, and other manufacturers continuously discharge wastewater containing dyes, which has become a global problem due to its risk when it enters the human and aquatic food chains [2]. This is due to the fact that, in dyes with organic structures, there are auxochromic and chromogenic groups, which limit the penetration of light into the water and have serious consequences in water bodies [3].

Contaminants of organic origins, such as biocides, dyes, surfactants, phenols, pharmaceuticals, and pesticides, are generally found in the aquatic environment [4]. Dyes are characterized by their resistance to degradation and can cause adverse effects on human

health and ecosystems [5]. Currently, about 40,000 dyes and pigments are in use, and approximately 7000 have different chemical structures. Among them, yellow 5, also known as tartrazine, is a petroleum-derived diazo anionic colorant, and it is extensively implemented in the food, cosmetic, and drug industries [6]. Yellow 5 was reported to be present in 20.5% of processed food products and 450 pharmaceutical products [7]. It is a highly water-soluble dye.

The study of the toxicological effects of tartrazine in mice showed that it is absorbed directly after ingestion in low proportions (10 mg/kg body weight (bw)/day) and that it degrades into metabolites in the colon [8]. As an azoic dye, it is associated with mutagenicity due to the generation of free amines in vivo through azo reduction. Furthermore, excessive ingestion above the 10 mg/kg bw/day limit established by the Joint FAO/WHO Expert Committee on Food Additives (JECFA) has been demonstrated [9]. It can cause allergic reactions; can cause potential damage to the liver, kidney function, lipid profiles; can cause carcinogenicity as well as genotoxic effects on the immune system; and can exacerbate hyperactivity. It can also cause respiratory and liver diseases as well as autoimmune diseases, such as lupus [8,10–12]. The excessive consumption of this contaminant not only has adverse effects on public health but also on the environment, as it persists in water and soil for extended periods, reducing soil fertility and the photosynthetic activity in aquatic plants by obstructing sunlight through the surface and impeding the penetration of O_2 [13,14]. Therefore, effluents containing this dye must undergo treatment processes before being discharged into surface water bodies. Consequently, the process of removing tartrazine in wastewater bodies presents a challenge due to its degradation-resistant structure [15]. Numerous treatment methods have been tested for the removal of the contaminants present in aqueous discharges, including biological processes, membrane processes, oxidation, chemical precipitation, and a growing application of biodegradable molecules [16–18]. Among these, adsorption is a technology commonly used for dye removal due to its low implementation cost, easy handling, high effectiveness, contaminant recovery, and material reusability [19,20]. For this reason, various natural resources have been studied for their use as adsorbent materials [21], such as yucca screening [22], mesoporous Ziziphus Spina-Christi [23], commercial granular materials, the biomass from rice husks [24], wheat straw residues [25], coconut and peanut shells [26], modified cellulose based on straw residues [27], pine needle waste [28], orange peels [29], and olive stones [30], among others. Among all the materials used, activated carbon is one of the most applied and effective but more expensive materials [31,32]. The current trend leans towards lignocellulosic-based adsorbent materials as an alternative [33], being agricultural residues that are a significant source for the synthesis of bioadsorbents, due to their low cost, high availability, and easy handling [34]. The focus on green adsorbents for their use as bioadsorbents is receiving considerable attention due to their renewability and accessibility [35]. Recently, various methods have been implemented for the adsorption of the dyes present in aqueous solutions, such as the use of modified activated carbons based on agricultural residues and nanocomponents [36] as well as the use of nanotechnology [37], nanomaterials [38], mesoporous materials [39], and activated biochar [40,41], among others.

Various experiments have been conducted using coconut residues for the adsorption of the dyes present in water bodies. In the study conducted by Filho et al. [42], the authors studied the performance of the coconut mesocarp as an adsorbent in the bleaching process of synthetic effluents containing reactive red dye 195. The results demonstrated that the coconut mesocarp achieved a removal efficiency of 89.92% for the dye present in the synthetic effluents. Likewise, in the study conducted by Tejada-Tovar et al. [43], they analyzed the effect of the adsorbent dosage and initial concentration on the removal of the azo-anionic dyes tartrazine and Congo red present in a synthetic aqueous solution using natural cellulose and modified cationic cellulose based on the coconut mesocarp. The results indicated that reducing the adsorbent dosage and increasing the initial concentration positively contributed to the adsorption capacity towards the dyes of both bioadsorbents, achieving a removal of 5.67 mg/g of tartrazine with natural cellulose and of 19.61 mg/g

with modified cationic cellulose. Meanwhile, for Congo red, 15.52 mg/g were removed with natural cellulose, and 19.99 mg/g were removed with modified cationic cellulose. In all cases, removal percentages higher than 97% were achieved with a quaternized biomass.

On the other hand, in the research conducted by Abdul Rahim et al. [44], the adsorption capacities of dried coconut waste were evaluated for the removal of azoic dyes from wastewater. The results demonstrated that dried coconut waste exhibited the highest adsorption capacity towards Congo red dye under pH 2 conditions, achieving a maximum adsorption capacity of 0.07 mmol/g. Cetyl trimethyl ammonium chloride (CTAC) was used to functionalize cellulose extracted from the coconut mesocarp for its assessment in the elimination of tartrazine; the new adsorbent, MCCR (i.e., modified coconut waste cellulose), was obtained, which showed efficient results with a 99% removal of the tartrazine in the solution, displaying a removal rate of 97% within the first 5 min and achieving equilibrium in 30 min, indicating a rapid process. When comparing these results with other materials found in the literature, a remarkable superiority was observed as in the case of the biomaterial synthesized from rice husks, which exhibited a removal efficiency of 90.45% [24]. Similarly, the material synthesized based on Moringa oleifera seeds showed a removal efficiency of 44% [45]. On the other hand, the material synthesized from orange peels showed an efficiency of 95% within 140 min [46]. Our study innovates by using CTAC as a surface-protonation agent for coconut cellulose, creating a highly effective adsorbent for the removal of tartrazine in solutions, and it is noteworthy that CTAC is not reported in the literature as a surface-protonating agent for the lignocellulosic biomaterials used to remove anionic dyes in aqueous solutions.

2. Materials and Methods

In the current study, a multilevel factorial experimental design was employed, consisting of 3 levels of adsorbent dosages, 3 variations of contaminant concentrations, 3 biomaterials, and 1 contaminant (tartrazine). Table 1 provides a more detailed overview of the experimental matrix.

Table 1. Experimental matrix.

Bioadsorbent Material	Adsorbent Dosage (mg)	Contaminant Concentration (ppm)
coconut shells (CSs)	15	40
	25	70
	35	100
coconut cellulose (CC)	15	40
	25	70
	35	100
modified coconut cellulose (MCC)	15	40
	25	70
	35	100

CTAC at 25% was used as a compound to treat cellulose. The synthetic solution of the colorant was prepared using analytical-grade tartrazine. The prepared materials underwent the zero-charge-point pH test. For this purpose, the pH of distilled water was adjusted within the range of 3–11 using 0.1 M NaOH and HCl. Subsequently, 5 mL of distilled water at various pH values was added to 10 mL centrifuge tubes. To the samples, a variable dosage of the prepared materials was added according to Table 1, and they were agitated for 24 h. After the elapsed time, the final pH was measured in each of the tubes and then was compared to the initial pH of each sample.

2.1. Coconut Shell Pretreatment

The coconut shells (CSs) were gathered in good condition to take advantage of their properties and to avoid early degradation. The material was washed with deionized water and was dried at 60 °C until constant mass was achieved. The size was classified in a shaker-type sieve shaker with stainless steel sieves, with mesh sizes of 8, 6.3, 4.75, 3.35, 2.362, 2, 1.7, 1, 0.5, and 0.355 mm [47]. The material was then stored in airtight bags.

2.2. Cellulose Extraction

The coconut cellulose (CC) was taken out by submerging 20 g of the pretreated coconut shell in distilled water, with a 4% *w*/*v* ratio, for 10 min with mechanical agitation at 300 rpm. The mixture was filtered, discarding the supernatant; the solid material was suspended in 0.5 L of NaOH at 4% w for 2 h at 200 rpm and 80 °C. The sample was rewashed and resuspended in a solution of NaOH. Then, it was washed again until water turned clear. The solid was treated by adding 50 g of $NaClO_2$ and 50 mL of glacial acetic acid to 0.5 L of distilled water; then, the mix was separated via decantation. The solid was washed until neutral pH was achieved and was dried at 60 °C [48].

2.3. Cellulose Quaternization

For the modification of cellulose, the method by Xu et al. [49] was used. This involved impregnating it with cetyl trimethylammonium chloride, which is a quaternary ammonium salt and an etherifying agent that alters the surface of cellulose. For this purpose, a ratio of 10 mL of cetyl trimethylammonium chloride at a concentration of 100 mmol/L was used for every 1 g of cellulose. The mixture was agitated on a shaker at 300 rpm for 24 h. The reaction did not require catalysis; once at a pH below 3, the reaction was then neutralized via thorough washing until achieving a pH of 7 or close to 7. The reaction between CTAC and CC is shown in Figure 1.

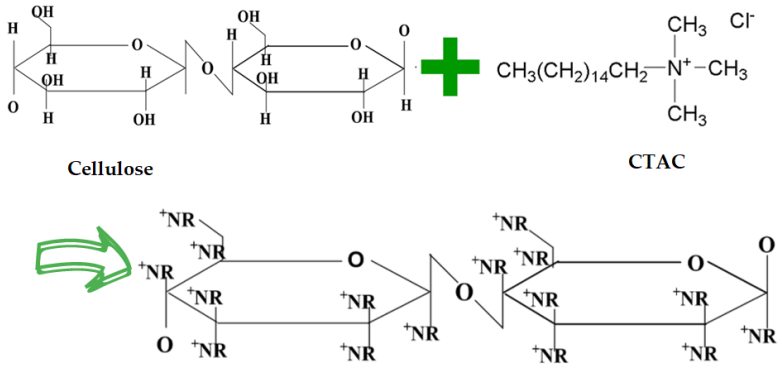

Figure 1. CC and CTAC reactions.

2.4. Characterization of Bioadsorbents

The synthetized biomaterials were characterized through the determination of the charge distribution on the bioadsorbent surface, which was performed by determining the zero-charge-point pH (pHpzc) [50]. Determination of dye concentration was carried out using a UV-VIS spectrophotometer, specifically the Biobase model BK-UV1900. The characterization of the adsorbent was performed using a Fourier-transform infrared spectrometer from Thermo Scientific (Waltham, MA, USA) (Nicolet 6700 FT-IR) (model: 912A0636) (serial: APW1100394) for the identification of the functional groups. The CC was characterized through thermogravimetric analysis (TGA) and through analysis via differential scanning calorimetry (DSC) with a TA Instruments SDT Q600 in nitrogen atmosphere at flow rate of 4 cm^3/min with temperature between 30 and 600 °C using a ramp function of 10 °C/min. Figure A1 shows images of the experimental results of the different stages.

2.5. Batch Adsorption Tests

A stock solution of tartrazine was prepared at 1000 mg/L. The adsorption experiments were developed by contacting 5 mL of dye solution with different doses of adsorbent in a Thermo Scientific MAXQ 4450 orbital agitator. The final concentration of tartrazine was measured via UV-Vis at 500 nm [51]. The removal effectiveness (%R) was calculated with Equation (1). The independent variables were considered to be the initial concentration and the adsorbent amount, and the response variable was the adsorption efficiency of the colorant tartrazine.

$$(\%)\ R = \left[\frac{C_0 - C_f}{C_0}\right] \times 100 \quad (1)$$

where C_0 (mg/L) is the initial concentration of dye in the solution and C_f (mg/L) is the final concentration of dye in the solution.

The statistical study was performed using Statgraphics Centurion XVIII.I.II software, establishing the influence of each of the independent variables over the removal efficiency; for this, ANOVA study, Pareto diagram, and response optimization were performed.

The influence of contact time was analyzed by taking samples at different time intervals (5, 10, 20, 30, 30, 60, 60, 120, 240, 480, 720, and 1440 min) at the best experimental condition of initial concentration and adsorbent dose found.

2.6. Adsorption Isotherms

Adsorption isotherms were stablished by fluctuating the initial concentration of tartrazine (25, 50, 75, 100, 125, and 150 ppm) at 150 rpm at room temperature [52] at the best condition of adsorbent dosage and contact time found experimentally. The experimental data were fitted to the Langmuir and Freundlich models [53,54] as shown in Table 2.

Table 2. Adsorption isotherm models.

Model	Equation	Parameters
Langmuir	$q_e = \frac{q_{max} b C_e}{1 + b C_e}$	q_{max} (mg/g): maximum amount of analyte removed per unit weight of biomass. b (L/mg): constant related to the affinity of binding sites to the contaminant. Ce (mg/L): concentration of the remaining contaminant in the solution.
Freundlich	$q_e = k_f C_e^{1/n}$	kf: indicator of adsorption capacity. n indicates the effect of concentration on adsorption capacity and represents the intensity of adsorption.

3. Results and Discussion

3.1. Characterization of Bioadsorbents

A thermogravimetric analysis provides information on the variation in a sample's composition with respect to the temperature and records the changes in its weight [55]. Figure 2 shows the TGA (thermogravimetric analysis) and DSC (differential scanning calorimetry) results of the cellulose extracted from the coconut mesocarp. A decrease of approximately 9.65% in the weight of the coconut mesocarp cellulose was observed between 75 °C and 140 °C, which was attributed to the moisture content present in the experimental sample. Additionally, a significant 50% mass loss was observed between 180 °C and 340 °C, corresponding to the degradation of hemicellulose and lignin [56]. Subsequently, above 340 °C, cellulose degradation occurred, with a degradation of 33.4% w. Between 400 and 600 °C, there was no significant decrease in the mass of the sample, which was associated with the absence of noncellulosic degradable substances, like lignin, and the possible presence of stable oxides at high temperatures [56,57].

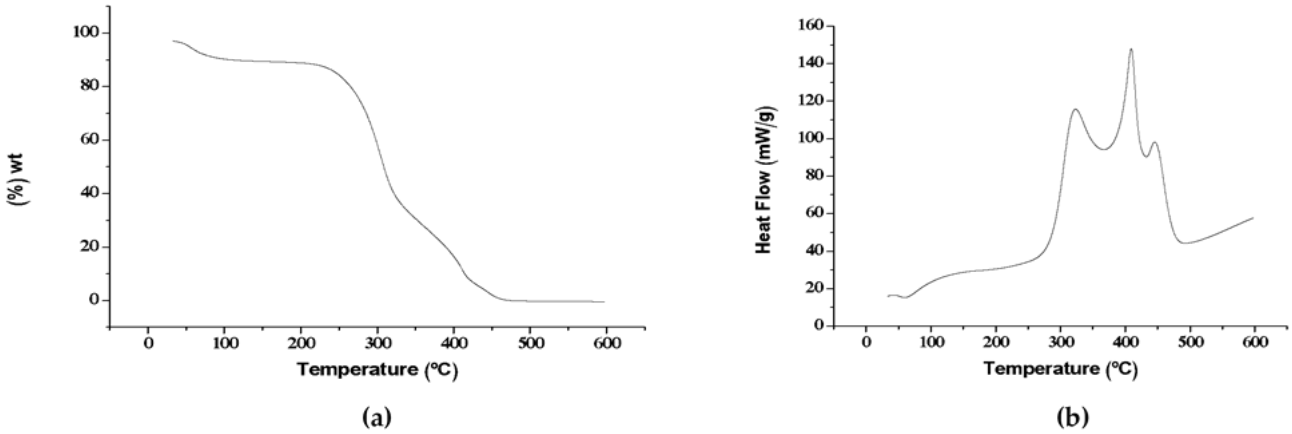

Figure 2. (**a**) TGA and (**b**) DSC analysis of cellulose extracted from coconut shell.

The DSC analysis shows that the obtained cellulose exhibited an endothermic peak around 80 °C, which was associated with water evaporation. From 320 to 350 °C, an exothermic pyrolysis reaction peak was observed, corresponding to the fusion of cellulose polymer crystals. The above observations may be linked to the different reaction mechanisms involved in the pyrolysis of the three components. The previous indications suggest that the carbonization process is highly exothermic, while volatilization is endothermic [58]. The absence of a peak between 222 and 228 °C indicates that hemicellulose was eliminated during the process of extracting the cellulose from the coconut mesocarp. This absence of a peak suggests that hemicellulose, which typically exhibits a distinct thermal decomposition behavior in this temperature range, had been effectively removed from the extracted cellulose sample [59].

From the FT-IR spectra (Figure 3), it can be said that, before the adsorption process, the bioadsorbents had the same type of spectrum. The structure of the CSs and MCC had more peaks than that of the CC. The following were observed: wide-ranging peaks of nearly 3730 cm^{-1}, 3482 cm^{-1}, and 3563 cm^{-1}, corresponding with the vibration of the OH and NHx- groups, respectively, present in cellulose and hemicellulose [60]. Amongst 3400 and 3500 cm^{-1} was the apparition of amines and carbonyls from the stretching vibrations of O-H. The band shown at 2904 cm^{-1} was caused by the C-H bonds of the hydrocarbon groups [58]. The wavelengths between 2000 and 2500 cm^{-1} showed faint signals from C≡C and C=O. From 1600 cm^{-1} onwards, a series of peaks was observed, which was attributed to the stretching vibration of C=O. These peaks were slightly milder in the CC and MCC. The characteristic band of cellulose was found in the zone between 1669 and 829 cm^{-1}, and it belonged to -CH_2 and -CH as well as -OH and C=O bonds. The band around 1418 cm^{-1} was related to the crystalline structure of cellulose; in contrast, the peak near 893 cm^{-1} corresponded to the amorphous region of cellulose [61]. After the adsorption of tartrazine, the CSs and MCC showed a shift in the bands between 3400 and 3800 cm^{-1} with respect to those before treatment as well as the broadening of the band between 2300 and 2500 cm^{-1}; this dissimilarity in the band was accredited to the existence of tartrazine in the bioadsorbent. In addition, the signals attributed to the dye structure at the wavenumber range of 1600–800 cm^{-1} could be seen, which confirmed its effective adsorption. Ranjbari et al. [62] reported that chitosan, functionalized with the ionic liquid Aliquat-366 and cetyltrimethylammonium bromide, showed changes in the alkyl group bands after the adsorption of tartrazine. The researchers attributed the adsorption mechanism to either weak electrostatic interactions or van der Waals forces. Goscianska and Ciesielczyk [63] conducted physicochemical studies to analyze the adsorbate/adsorbent interactions, determining that tartrazine partially replaced the surface groups of the adsorbent through the formation of hydrogen bonds.

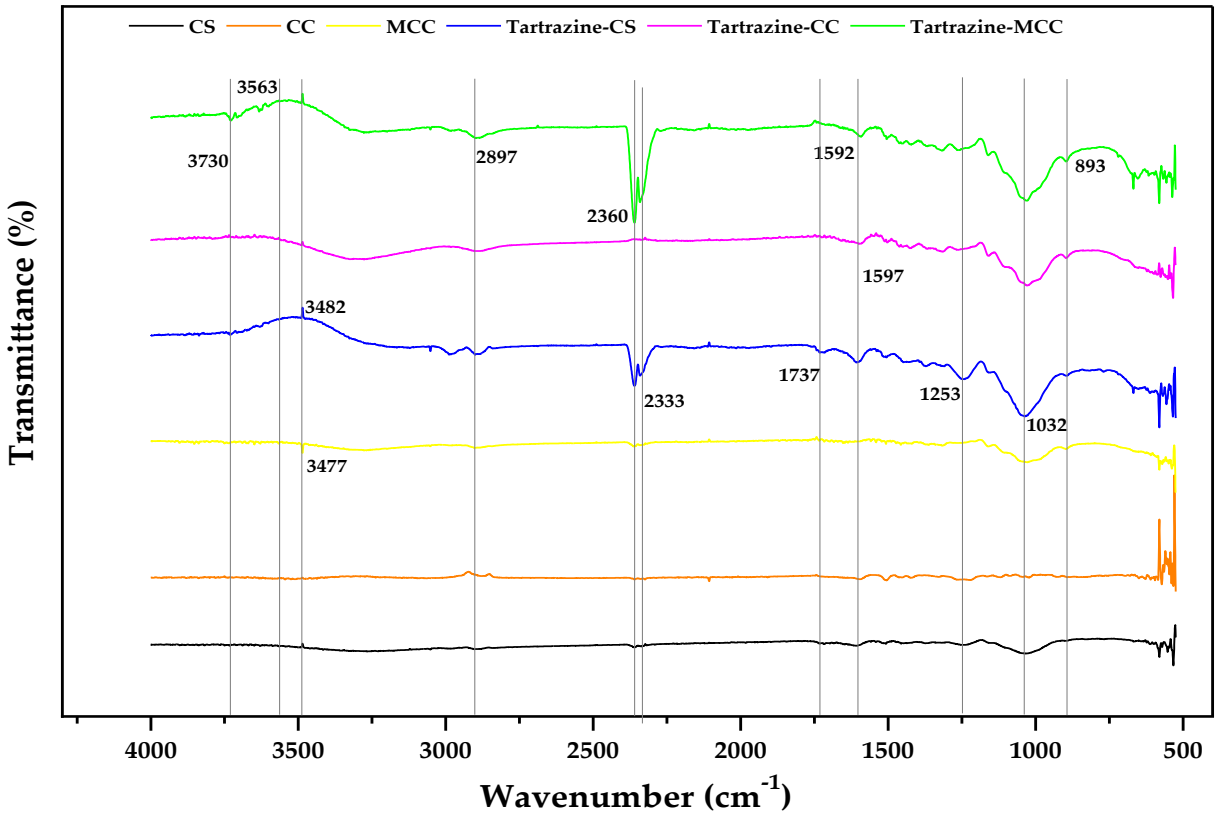

Figure 3. Normalized FTIR spectra of coconut-shell-based bioadsorbents before and after tartrazine removal.

3.2. pH Point of Zero Charge

The point at which the bioadsorbents exhibited a net charge of zero was determined using the pH_{PZC} [64]. Table 3 recaps the results of the bioadsorbents under study.

Table 3. pHpzc of the bioadsorbents from coconut shell.

Bioadsorbent	pH_{PZC}
Coconut shell	7.27
Coconut shell cellulose	5.88
CTAC-modified coconut shell cellulose	5.73

It was observed that the crude biomass presented the highest pH_{PZC}, which was close to basicity. As modifications were made to the chemical structure of the pristine biomaterial, this parameter decreased. It can be seen that the cellulose had a pH_{PZC} of 5.88; this is in the pH range for raw cellulose (5.0–7.5) [65]. When it was chemically modified with cetyl trimethyl ammonium chloride, its pH slightly decreased, which can be explained by the fact that impregnation with this chemical reagent does not considerably affect the distribution of the electrical charges on the surface of cellulose. Considering the pH_{PZC} results, it was stablished that the experimental pH for the tartrazine removal experiments in this study would be 4 for the three adsorbents; considering that the adsorbents behaved as an ion exchange matrix that would be protonated at $pH < pH_{PZC}$, the external surface of the material might therefore be protonated and attract the dye metabolites through electrostatic forces [66,67].

3.3. Effect of Adsorbent Dosage and Initial Concentration

Figure 4 shows that the CSs and CC presented adsorption yields between 1.09 and 17.31% at the different conditions of initial concentrations evaluated, with a better performance from the CC. This was because the surface of the bioadsorbents exhibited the coexistence of positive and negative charges due to the influence of the pHpzc [68]. It was also observed that, as the tartrazine concentration increased, as did the removal efficiency; this was because desorption was lower due to the fact that the concentration gradient became smaller [69]. This performance from the CSs and CC suggests the need for the modification of the biomaterials to enhance the adsorption capacity of the biomaterials.

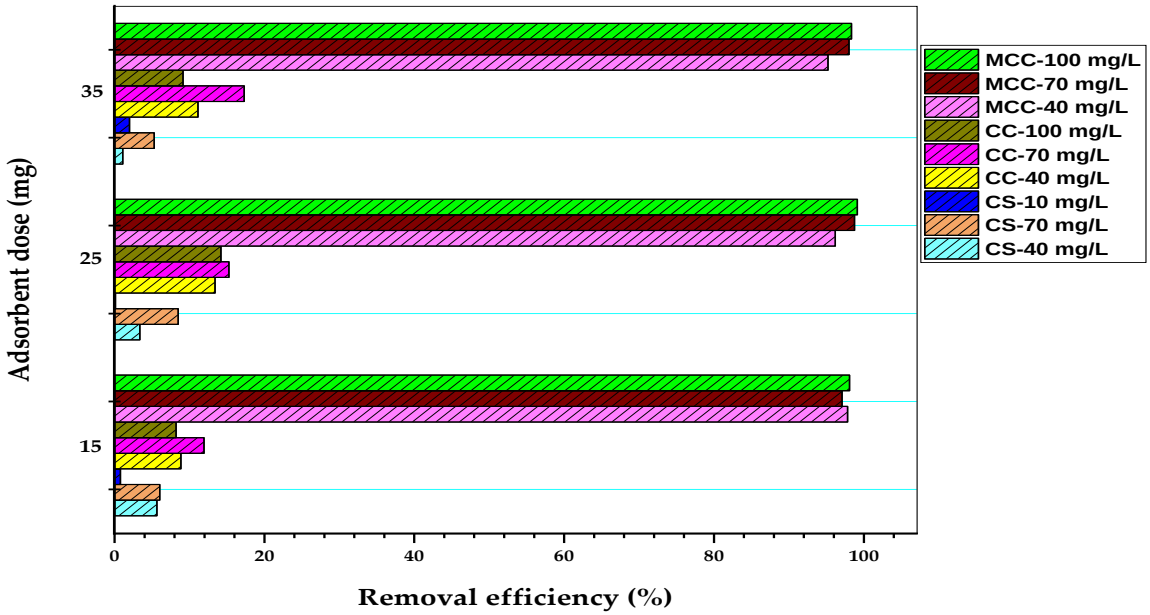

Figure 4. Effect of adsorbent dose and initial tartrazine concentration on removal efficiency in mm.

Regarding the MCC, it was found that the removal efficiency was in the range of 95.22 to 99.12%, finding a positive effect of the initial concentration of tartrazine and dismissing the processes resistant to diffusion and the mass transfer from the bulk of the solution. It was also observed that the rise in the amount of adsorbent produced a growth in the removal percentage because of the augmentation of the active sites on the adsorbent [70]. Although the initial concentration effect on the removal of tartrazine was positive, an antagonistic phenomenon of the adsorbent dose in terms of the adsorption capacity was obtained due to the split in the concentration gradient between the solute concentration in the solution and on the adsorbent surface [62]. Consequently, there was competition for solute ions for limited available active sites and other superficial phenomena due to charge equilibrium interactions [63]. The data for the above results can also be seen in more detail in Table A1.

When using 50 mg of the adsorbent, a decrease in the efficiency of tartrazine removal was reported, as the initial concentration of tartrazine in the solution increased from 50 mg/L to 250 mg/L. This decrease in efficiency can be attributed to maintaining a constant adsorbent dosage, resulting in a fixed number of active sites available for adsorption. It was suggested that, at low dye concentrations, the abundant active sites of the adsorbent material could adsorb a greater amount of the target analyte. However, as the dye concentration increased, the active sites became saturated, leading to a reduced removal of tartrazine [53]. Similar results were reported when using a rice husk and granular activated carbon with 0.1 g of adsorbent in 50 mL of solution, as the tartrazine concentration increased from 5 mg/L to 50 mg/L. This phenomenon was attributed to the saturation of the adsorbent surface at the adsorption sites, likely due to the formation of a monolayer of dye molecules at the interface with the adsorbent [71]. Thus, it can be

suggested that, within a higher concentration range, fractional removal is always greater, whereas, for lower concentration ranges, the percentage of dye removal is higher [72].

On the other hand, concerning the adsorbent dosage, it has been reported that increasing the amount of material enhances the adsorption process of tartrazine, which is consistent with the results of the current study at different evaluated initial concentrations. As the amount of the rice husk and granular activated carbon increased between 0.0125 g and 0.4 g in 50 mL, an increase in the removal efficiency was observed. This can be attributed to the larger contact area between the anion and the active sites, resulting in a higher number of available adsorption centers. Consequently, a greater amount of adsorption centers led to an improved efficiency of tartrazine removal from the solution [73].

From the analysis of variance in Table 4, it was determined that the initial concentration was the variable with the highest statistical influence on the removal efficiency [74].

Table 4. ANOVA of the removal efficiency towards tartrazine of bioadsorbents prepared from coconut shell.

Source	Bioadsorbents								
	CS			CC			MCC		
	Sum of Squares	F-Ratio	*p*-Value	Sum of Squares	F-Ratio	*p*-Value	Sum of Squares	F-Ratio	*p*-Value
A: Adsorbent dosage	3.3227	1.44	0.32	12.22	2.88	0.19	0.33	0.42	0.56
B: Initial concentration	16.30	7.05	0.077	0.58	0.14	0.74	6.65	8.52	0.06
AA	3.66	1.58	0.29	20.39	4.80	0.12	0.71	0.91	0.41
AB	8.27	3.58	0.16	0.47	0.11	0.76	2.04	2.61	0.20
BB	33.65	14.55	0.032	32.17	7.57	0.07	0.47	0.60	0.49
Total error	6.94			12.74			2.34		
Total (corr.)	72.15			78.55			12.55		

3.4. Effect of the Time

The adsorption speed was important for the design of the batch experiments for the practical application of the adsorbent. The effect of the contact time was evaluated, showing the adsorption capacity (qt) vs. the time (min) (Figure 5).

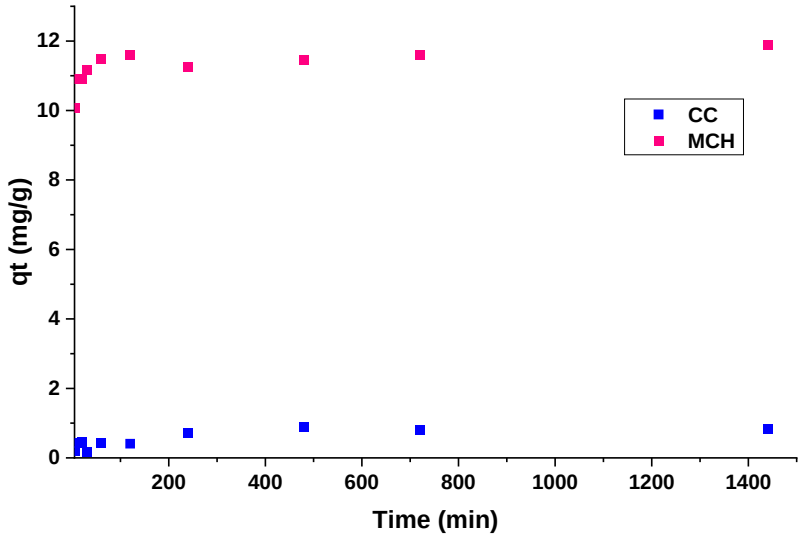

Figure 5. Effect of the contact time.

About 97% of tartrazine was removed in the first 5 min using the CC and MCC, and the equilibrium time was close to 30 min, which guaranteed the fast adsorption of the contaminant. The MCC had an adsorption capacity of 11.89 mg/g at equilibrium, while that of the CC was 0.85 mg/g. It can be said that adsorption happened in two phases: first was the fast stage controlled via intraparticle diffusion from the bulk to the adsorbent surface, and after that was the slower step until the equilibrium subject to mass transfer was reached [75].

Alike results have been described for the elimination of tartrazine in defatted soybeans and bottom ash; here, the establishment of an equilibrium took about 3–4 h [76]. When using bioadsorbents prepared from moringa seeds, there was an equilibrium time of around 600 min, a removal efficiency of 99%, and adsorption capacities between 3.3 and 3.9 mg/g [23], which were lower than those obtained in this study for the MCC. When using cellulose modified by hyperbranched polyethylenimine to remove anionic reactive yellow, bright cationic yellow, and nonionic dispersed brown, equilibrium times were obtained between 120 and 180 min, with a rapid increase in the first 30 min of the study [77].

3.5. Adsorption Equilibrium

From the data in Table 5, the adsorption of tartrazine using the CC and MCC was adjusted by the Freundlich model, having a slight variation with respect to the Langmuir model. This indicates that the process was given by physical and chemical adsorption with the formation of mono- and multilayers due to the heterogeneity of the sorption sites. In addition, the limiting step was the creation of multilayers. Strong bonds first occupied the active adsorption sites, and this strength decreased as they were occupied by ions [78]. For detailed isotherm parameter data with the Freundlich and Langmuir models, see Tables A2–A5.

Table 5. Adsorption isotherm parameters.

Model	Parameters	Bioadsorbent	
		CC	MCC
Langmuir	q_{max} (mg/g)	5.222	18.412
	b (L/mg)	2.0967×10^{-5}	1.220×10^{-4}
	R^2	0.933	0.914
Freundlich	k_f	0.033	0.956
	n	0.937	0.973
	R^2	0.936	0.915

It was observed that k_f exhibited an MCC > CC behavior (Table 5); it was intuited that the active centers of the MCC were more affine with tartrazine than those of the CC. This was due to the protonation of the MCC surface after the chemical treatment with CTAC [79]. The values of '*n*' were < 1–10; therefore, the chemical interactions between tartrazine and the active sites were weak [24]. When using bentonite modified with hexadecyltrimethylammonium bromide for the removal of tartrazine, the Freundlich model fitted the isotherm data [5]; similar results were found when activated charcoal from *Lantana camara* [76] was evaluated in the remotion of the dye, while for the use of activated carbon from Moringa [80], the Langmuir model was found to be a better fit.

Previously, values of the Langmuir parameter q_{max} were obtained for the removal of tartrazine with respect to adsorbents of a different nature. The results obtained in the present study when using the MCC were superior when using babassu bone activated carbon (11.99 mg/g) [80] and coconut shells [59]. However, superior results have been obtained when using modifications with reagents and adsorbents of a different nature, such as bentonite modified with hexadecyltrimethylammonium bromide (40.79) [5], H_3PO_4-modified corncob activated carbon (89.75) [81], and a chitozan/polyaniline nanocomposite (617.8) [52].

4. Conclusions

The synthesized bioadsorbents exhibited a complex structure with the presence of multiple active adsorption sites. This suggests that these materials possess a high potential for effectively removing contaminants from wastewater. Increasing the initial concentration of tartrazine in a solution had a positive impact on the removal efficiency. Notably, the modified coconut cellulose (MCC) bioadsorbent achieved an impressive 99% removal efficiency, highlighting its effectiveness as an adsorbent. The adsorption process showed rapid initial removal kinetics, with approximately 97% of the dye being removed within the first 5 min. The equilibrium point was reached at 30 min, indicating that the adsorption process stabilized relatively quickly.

Both the Langmuir and Freundlich models provided a satisfactory fit to the adsorption isotherm data. This implies that the adsorption mechanism involves both physical and chemical interactions, making the process more versatile and efficient. The modified coconut shell bioadsorbent is particularly noteworthy, as it demonstrated an excellent performance in removing tartrazine from aqueous solutions. This further supports the potential application of the MCC as an efficient and ecofriendly adsorbent for wastewater treatment.

Author Contributions: Experimental data, F.A.-B. and Y.P.-M.; conceptualization, C.T.-T. and Á.V.-O.; methodology, C.T.-T.; software, Á.D.G.-D.; validation, Á.D.G.-D.; formal analysis, Á.D.G.-D.; investigation, C.T.-T.; data curation, Á.V.-O.; writing—original draft preparation, C.T.-T.; writing—review and editing, Á.D.G.-D.; visualization, Á.D.G.-D.; supervision, C.T.-T.; project administration, C.T.-T. All authors have read and agreed to the published version of the manuscript.

Funding: This research received no external funding.

Data Availability Statement: The data that support the findings of this study are available from the corresponding author upon reasonable request.

Acknowledgments: The authors thank to the Universidad de Cartagena for providing the materials, equipment, and laboratory facilities required to successfully conclude this research project.

Conflicts of Interest: The authors declare no conflict of interest.

Appendix A

Table A1. Tartrazine adsorption results for coconut mesocarp.

Biomass	Adsorbent Dosage (mg)	Initial Concentration (ppm)	Final Concentration (ppm)	% Removal	Qt
Coconut shell	15	39.88	37.6233766	5.65853404	0.45132468
	25	39.88	38.5324675	3.37896807	0.1617039
	35	39.88	39.4415584	1.0994021	0.03758071
	15	68.79	64.6363636	6.03813979	0.83072727
	25	68.79	62.9480519	8.49243793	0.70103377
	35	68.79	65.1558442	5.28297114	0.31149907
	15	98.01	97.2337662	0.79199446	0.15524675
	25	98.01	97.8831169	0.12945936	0.01522597
	35	98.01	96.0649351	1.98455763	0.16671985
Coconut cellulose	15	39.88	36.4545455	8.58940458	0.68509091
	25	39.88	34.6363636	13.1485365	0.62923636
	35	39.88	35.5454545	10.8689705	0.37153247
	15	68.79	61.6493506	10.3803596	1.42812987
	25	68.79	59.3116883	13.7786185	1.1373974
	35	68.79	57.8831169	15.8553323	0.9348757
	15	98.01	91.7792208	6.35728928	1.24615584
	25	98.01	85.8051948	12.4526122	1.46457662
	35	98.01	90.8701299	7.28483841	0.61198887

Table A1. *Cont.*

Biomass	Adsorbent Dosage (mg)	Initial Concentration (ppm)	Final Concentration (ppm)	% Removal	Qt
Modified coconut cellulose	15	39.88	0.87012987	97.8181297	7.80197403
	25	39.88	1.51948052	96.1898683	4.60326234
	35	39.88	1.90909091	95.2129115	3.25464935
	15	68.79	2.03896104	97.035963	13.3502078
	25	68.79	0.87012987	98.7350925	8.15038442
	35	68.79	1.38961039	97.9799238	5.77717625
	15	98.01	1.90909091	98.0521468	19.2201818
	25	98.01	0.87012987	99.112203	11.6567844
	35	98.01	1.64935065	98.3171609	8.25948423

Table A2. Langmuir isotherm parameters for adsorption of tartrazine by cellulose from coconut mesocarp.

Equation	**Q = (qmax × (b × C))/(1 + (b × C))**		
R^2	**0.93263**		
		Value	**Standard Error**
Qe	Qmax	2151.22167	250,240.23045
Qe	B	2.0967×10^{-5}	0.00244

Table A3. Freundlich isotherm parameters for adsorption of tartrazine by cellulose from coconut mesocarp.

Equation	**Q = kf × (C(1/n))**		
R^2	**0.93557**		
		Value	**Standard Error**
Qe	Kf	0.03345	0.02537
Qe	N	0.93716	0.1521

Table A4. Freundlich isotherm parameters for adsorption of tartrazine by modified cellulose from wheat milling residues.

Equation	**Q = (qmax × (b × C))/(1 + (b × C))**		
R^2	**−0.25**		
		Value	**Standard Error**
Qe	Qmax	9.6761	2.85096
Qe	B	4.34896×10^{34}	--

Table A5. Freundlich isotherm parameters for adsorption of tartrazine by modified cellulose from coconut mesocarp.

Equation	**Q = kf × (C(1/n))**		
R^2	**−0.25**		
		Value	**Standard Error**
Qe	Kf	9.6761	2.85096
Qe	N	3.48385×10^{24}	--

Appendix B

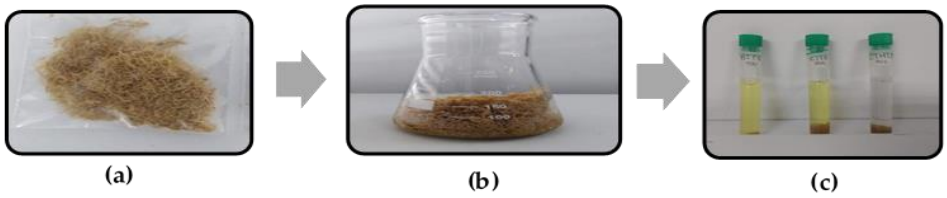

Figure A1. (**a**) Coconut cellulose, (**b**) cellulose quaternization, and (**c**) cellulose and cellulose-modified tartrazine.

References

1. Liu, W.; Wu, C.-H.; Blanco, Á.; Qian, C.; Gao, Y.; Chen, L. Green Supply Chain Circular Economy Evaluation System Based on Industrial Internet of Things and Blockchain Technology under ESG Concept. *Processes* **2023**, *11*, 1999. [CrossRef]
2. Singh, H.; Goyal, A.; Bhardwaj, S.K.; Khatri, M.; Bhardwaj, N. Highly robust UiO-66@PVDF metal–organic framework beads for tartrazine removal from aqueous solutions. *Mater. Sci. Eng. B* **2023**, *288*, 116165. [CrossRef]
3. Jabeen, A.; Bhatti, H.N. Adsorptive removal of reactive green 5 (RG-5) and direct yellow 50 (DY-50) from simulated wastewater by *Mangifera indica* seed shell and its magnetic composite: Batch and Column study. *Environ. Technol. Innov.* **2021**, *23*, 101685. [CrossRef]
4. Sousa, J.C.G.; Ribeiro, A.R.; Barbosa, M.O.; Pereira, M.F.R.; Silva, A.M.T. A review on environmental monitoring of water organic pollutants identified by EU guidelines. *J. Hazard. Mater.* **2018**, *344*, 146–162. [CrossRef] [PubMed]
5. Otavo-Loaiza, R.A.; Sanabria-González, N.R.; Giraldo-Gómez, G.I. Tartrazine Removal from Aqueous Solution by HDTMA-Br-Modified Colombian Bentonite. *Sci. World J.* **2019**, *2019*, 2042563. [CrossRef]
6. Rovina, K.; Siddiquee, S.; Shaarani, S.M. A Review of Extraction and Analytical Methods for the Determination of Tartrazine (E 102) in Foodstuffs. *Crit. Rev. Anal. Chem.* **2017**, *47*, 309–324. [CrossRef]
7. Batada, A.; Jacobson, M.F. Prevalence of Artificial Food Colors in Grocery Store Products Marketed to Children. *Clin. Pediatr.* **2016**, *55*, 1113–1119. [CrossRef]
8. Bastaki, M.; Farrell, T.; Bhusari, S.; Pant, K.; Kulkarni, R. Lack of genotoxicity in vivo for food color additive Tartrazine. *Food Chem. Toxicol.* **2017**, *105*, 278–284. [CrossRef]
9. World Health Organization. JECFA Evaluation of Certain Food Additives: Eighty-Second Report of the Joint FAO/WHO Expert Committee on Food Additives. 2016. Available online: https://apps.who.int/iris/handle/10665/250277 (accessed on 20 March 2022).
10. Amin, K.A.; Al-Shehri, F.S. Toxicological and safety assessment of tartrazine as a synthetic food additive on health biomarkers: A review. *African J. Biotechnol.* **2018**, *17*, 139–149. [CrossRef]
11. Khayyat, L.; Essawy, A.; Sorour, J.; Soffar, A. Tartrazine induces structural and functional aberrations and genotoxic effects in vivo. *PeerJ* **2017**, *2017*, 1–14. [CrossRef]
12. Gičević, A.; Hindija, L.; Karačić, A. Toxicity of azo dyes in pharmaceutical industry. *IFMBE Proc.* **2019**, *73*, 581–587.
13. Al-Tohamy, R.; Ali, S.S.; Li, F.; Okasha, K.M.; Mahmoud, Y.A.G.; Elsamahy, T.; Jiao, H.; Fu, Y.; Sun, J. A critical review on the treatment of dye-containing wastewater: Ecotoxicological and health concerns of textile dyes and possible remediation approaches for environmental safety. *Ecotoxicol. Environ. Saf.* **2022**, *231*, 113160. [CrossRef] [PubMed]
14. De Lima Barizão, A.C.; Silva, M.F.; Andrade, M.; Brito, F.C.; Gomes, R.G.; Bergamasco, R. Green synthesis of iron oxide nanoparticles for tartrazine and bordeaux red dye removal. *J. Environ. Chem. Eng.* **2020**, *8*, 103618. [CrossRef]
15. Perveen, S.; Nadeem, R.; Nosheen, F.; Asjad, M.I.; Awrejcewicz, J.; Anwar, T. Biochar-Mediated Zirconium Ferrite Nanocomposites for Tartrazine Dye Removal from Textile Wastewater. *Nanomaterials* **2022**, *12*, 2828. [CrossRef]
16. Petrie, B.; Barden, R.; Kasprzyk-Hordern, B. A review on emerging contaminants in wastewaters and the environment: Current knowledge, understudied areas and recommendations for future monitoring. *Water Res.* **2015**, *72*, 3–27. [CrossRef]
17. Rodriguez-Narvaez, O.M.; Peralta-Hernandez, J.M.; Goonetilleke, A.; Bandala, E.R. Treatment technologies for emerging contaminants in water: A review. *Chem. Eng. J.* **2017**, *323*, 361–380. [CrossRef]
18. Porri, A.; Baroncelli, R.; Guglielminetti, L.; Sarrocco, S.; Guazzelli, L.; Forti, M.; Catelani, G.; Valentini, G.; Bazzichi, A.; Franceschi, M.; et al. *Fusarium oxysporum* degradation and detoxification of a new textile-glycoconjugate azo dye (GAD). *Fungal Biol.* **2011**, *115*, 30–37. [CrossRef]
19. Adegoke, K.A.; Bello, O.S. Dye sequestration using agricultural wastes as adsorbents. *Water Resour. Ind.* **2015**, *12*, 8–24. [CrossRef]
20. Singh, N.B.; Nagpal, G.; Agrawal, S. Rachna Water purification by using Adsorbents: A Review. *Environ. Technol. Innov.* **2018**, *11*, 187–240. [CrossRef]
21. Zhou, Y.; Zhang, M.; Wang, X.; Huang, Q.; Min, Y.; Ma, T.; Niu, J. Removal of Crystal Violet by a Novel Cellulose-Based Adsorbent: Comparison with Native Cellulose. *Ind. Eng. Chem. Res.* **2014**, *53*, 5498–5506. [CrossRef]
22. Chukwuemeka-Okorie, H.O.; Ekuma, F.K.; Akpomie, K.G.; Nnaji, J.C.; Okereafor, A.G. Adsorption of tartrazine and sunset yellow anionic dyes onto activated carbon derived from cassava sievate biomass. *Appl. Water Sci.* **2021**, *11*, 27. [CrossRef]

23. Fennouh, R.; Benturki, O.; Mokhati, A.; Benturki, A.; Belhamdi, B.; Trari, M. Preparation and characterization of highly mesoporous activated carbon from Ziziphus Spina-Christi for tartrazine adsorption from a simulated effluent. *Biomass Convers. Biorefinery* 2023. [CrossRef]
24. Khader, E.H.; Mohammed, T.J.; Albayati, T.M. Comparative performance between rice husk and granular activated carbon for the removal of azo tartrazine dye from aqueous solution. *Desalin. Water Treat.* **2021**, *229*, 372–383. [CrossRef]
25. Ortega-Toro, R.; Tejada-Tovar, C.; Villabona-Ortíz, A.; Aguilar-Bermúdez, F.; Pájaro-Moreno, Y. Effective adsorption of Tartrazine by modified biomaterial from wheat residues. *Ing. Compet.* **2022**, *24*, 1. [CrossRef]
26. Ademoriyo, C.; Enyoh, C. Batch Adsorption Studies of Sunset Yellow and Tartrazine Using Coconut and Groundnut Shells. *J. Biomed. Res. Environ. Sci.* **2020**, *1*, 163–172. [CrossRef]
27. Villabona-Ortíz, Á.; Figueroa-Lopez, K.J.; Ortega-Toro, R. Kinetics and Adsorption Equilibrium in the Removal of Azo-Anionic Dyes by Modified Cellulose. *Sustainability* **2022**, *14*, 3640. [CrossRef]
28. Pandey, D.; Daverey, A.; Dutta, K.; Yata, V.K.; Arunachalam, K. Valorization of waste pine needle biomass into biosorbents for the removal of methylene blue dye from water: Kinetics, equilibrium and thermodynamics study. *Environ. Technol. Innov.* **2022**, *25*, 102200. [CrossRef]
29. Karaman, C.; Karaman, O.; Show, P.L.; Karimi-Maleh, H.; Zare, N. Congo red dye removal from aqueous environment by cationic surfactant modified-biomass derived carbon: Equilibrium, kinetic, and thermodynamic modeling, and forecasting via artificial neural network approach. *Chemosphere* **2022**, *290*, 133346. [CrossRef]
30. Al-Ghouti, M.A.; Al-Absi, R.S. Mechanistic understanding of the adsorption and thermodynamic aspects of cationic methylene blue dye onto cellulosic olive stones biomass from wastewater. *Sci. Rep.* **2020**, *10*, 15928. [CrossRef] [PubMed]
31. Mahmoud, M.E.; Abdelfattah, A.M.; Tharwat, R.M.; Nabil, G.M. Adsorption of negatively charged food tartrazine and sunset yellow dyes onto positively charged triethylenetetramine biochar: Optimization, kinetics and thermodynamic study. *J. Mol. Liq.* **2020**, *318*, 114297. [CrossRef]
32. Martini, B.K.; Daniel, T.G.; Corazza, M.Z.; De Carvalho, A.E. Methyl orange and tartrazine yellow adsorption on activated carbon prepared from boiler residue: Kinetics, isotherms, thermodynamics studies and material characterization. *J. Environ. Chem. Eng.* **2018**, *6*, 6669–6679. [CrossRef]
33. Kumari, S.; Mankotia, D.; Chauhan, G.S. Crosslinked cellulose dialdehyde for Congo red removal from its aqueous solutions. *J. Environ. Chem. Eng.* **2016**, *4*, 1126–1136. [CrossRef]
34. Sharma, A.; Siddiqui, Z.M.; Dhar, S.; Mehta, P.; Pathania, D. Adsorptive removal of congo red dye (CR) from aqueous solution by *Cornulaca monacantha* stem and biomass-based activated carbon: Isotherm, kinetics and thermodynamics. *Sep. Sci. Technol.* **2018**, *54*, 916–929. [CrossRef]
35. Tan, C.H.C.; Sabar, S.; Hussin, M.H. Development of immobilized microcrystalline cellulose as an effective adsorbent for methylene blue dye removal. *South African J. Chem. Eng.* **2018**, *26*, 11–24. [CrossRef]
36. Foroutan, R.; Peighambardoust, S.J.; Peighambardoust, S.H.; Pateiro, M.; Lorenzo, J.M. Adsorption of crystal violet dye using activated carbon of lemon wood and activated carbon/fe3 o4 magnetic nanocomposite from aqueous solutions: A kinetic, equilibrium and thermodynamic study. *Molecules* **2021**, *26*, 2241. [CrossRef]
37. Osagie, C.; Othmani, A.; Ghosh, S.; Malloum, A.; Kashitarash Esfahani, Z.; Ahmadi, S. Dyes adsorption from aqueous media through the nanotechnology: A review. *J. Mater. Res. Technol.* **2021**, *14*, 2195–2218. [CrossRef]
38. Kaci, M.M.; Nasrallah, N.; Djaballah, A.M.; Akkari, I.; Belabed, C.; Soukeur, A.; Atmani, F.; Trari, M. Insights into the optical and electrochemical features of $CuAl_2O_4$ nanoparticles and it use for methyl violet oxidation under sunlight exposure. *Opt. Mater.* **2022**, *126*, 112198. [CrossRef]
39. Alardhi, S.M.; Albayati, T.M.; Alrubaye, J.M. Adsorption of the methyl green dye pollutant from aqueous solution using mesoporous materials MCM-41 in a fixed-bed column. *Heliyon* **2020**, *6*, e03253. [CrossRef]
40. Akkari, I.; Spessato, L.; Graba, Z.; Bezzi, N.; Kaci, M.M. A sustainably produced hydrochar from pomegranate peels for the purification of textile contaminants in an aqueous medium. *Sustain. Chem. Pharm.* **2023**, *31*, 100924. [CrossRef]
41. Akkari, I.; Graba, Z.; Pazos, M.; Bezzi, N.; Atmani, F.; Manseri, A.; Kaci, M.M. Recycling waste by manufacturing biomaterial for environmental engineering: Application to dye removal. *Biocatal. Agric. Biotechnol.* **2023**, *50*, 102709. [CrossRef]
42. Filho, A.; Aroucha, E.; Leite, R.; Dos Santos, F. Evaluation of adsortive potential of coconut mesocarp in the removal of reactive red dye 195 in aqueous effluents. *Rev. Mater.* **2020**, *25*, 1–9. [CrossRef]
43. Tejada-Tovar, C.; Villabona-Ortiz, Á.; Gonzalez-Delgado, Á.D. Adsorption of Azo-Anionic Dyes in a Solution Using Modified Coconut (*Cocos nucifera*) Mesocarp: Kinetic and Equilibrium Study. *Water* **2021**, *13*, 1382. [CrossRef]
44. Abdul, R.; Mohsin, H.; Chin, K.; Johari, K.; Saman, N. Promising Low-cost Adsorbent from Desiccated Coconut Waste for Removal of Congo Red Dye from Aqueous Solution. *Water. Air. Soil Pollut.* **2021**, *232*, 357. [CrossRef]
45. Reck, I.M.; Paixão, R.M.; Bergamasco, R.; Vieira, M.F.; Vieira, A.M.S. Investigation of *Moringa oleifera* seeds as effective and low-cost adsorbent to remove yellow dye tartrazine in fixed-bed column. *Sep. Sci. Technol.* **2020**, *55*, 13–25. [CrossRef]
46. Amin, M.T.; Alazba, A.A.; Shafiq, M. Comparative study for adsorption of methylene blue dye on biochar derived from orange peel and banana biomass in aqueous solutions. *Environ. Monit. Assess.* **2019**, *191*, 735. [CrossRef]
47. Han, Y.; Cao, X.; Ouyang, X.; Sohi, S.P.; Chen, J. Adsorption kinetics of magnetic biochar derived from peanut hull on removal of Cr (VI) from aqueous solution: Effects of production conditions and particle size. *Chemosphere* **2016**, *145*, 336–341. [CrossRef]

48. Xu, J.; Krietemeyer, E.F.; Boddu, V.M.; Liu, S.X.; Liu, W.C. Production and characterization of cellulose nanofibril (CNF) from agricultural waste corn stover. *Carbohydr. Polym.* **2018**, *192*, 202–207. [CrossRef]
49. Xu, J.h.; Gao, N.y.; Deng, Y.; Sui, M.h.; Tang, Y.l. Perchlorate removal by granular activated carbon coated with cetyltrimethyl ammonium bromide. *J. Colloid Interface Sci.* **2011**, *357*, 474–479. [CrossRef]
50. Herrera-Barros, A.; Tejada-Tovar, C.; Villabona-Ortíz, A.; Gonzalez-Delgado, A.D.; Benitez-Monroy, J. Cd (II) and Ni (II) uptake by novel biosorbent prepared from oil palm residual biomass and Al_2O_3 nanoparticles. *Sustain. Chem. Pharm.* **2020**, *15*, 100216. [CrossRef]
51. Alcantara-Cobos, A.; Gutiérrez-Segura, E.; Solache-Ríos, M.; Amaya-Chávez, A.; Solís-Casados, D.A. Tartrazine removal by ZnO nanoparticles and a zeolite-ZnO nanoparticles composite and the phytotoxicity of ZnO nanoparticles. *Microporous Mesoporous Mater.* **2020**, *302*, 110212. [CrossRef]
52. Sahnoun, S.; Boutahala, M. Adsorption removal of tartrazine by chitosan/polyaniline composite: Kinetics and equilibrium studies. *Int. J. Biol. Macromol.* **2018**, *114*, 1345–1353. [CrossRef] [PubMed]
53. Mittal, A.; Kurup, L.; Mittal, J. Freundlich and Langmuir adsorption isotherms and kinetics for the removal of Tartrazine from aqueous solutions using hen feathers. *J. Hazard. Mater.* **2007**, *146*, 243–248. [CrossRef] [PubMed]
54. Al-Ghouti, M.A.; Da'ana, D.A. Guidelines for the use and interpretation of adsorption isotherm models: A review. *J. Hazard. Mater.* **2020**, *393*, 122383. [CrossRef]
55. Jiang, Z.; Hu, D. Molecular mechanism of anionic dyes adsorption on cationized rice husk cellulose from agricultural wastes. *J. Mol. Liq.* **2019**, *276*, 105–114. [CrossRef]
56. Herlina Sari, N.; Wardana, I.N.G.; Irawan, Y.S.; Siswanto, E. Characterization of the Chemical, Physical, and Mechanical Properties of NaOH-treated Natural Cellulosic Fibers from Corn Husks. *J. Nat. Fibers* **2017**, *15*, 545–558. [CrossRef]
57. Fan, C.; Zhang, Y. Adsorption isotherms, kinetics and thermodynamics of nitrate and phosphate in binary systems on a novel adsorbent derived from corn stalks. *J. Geochemical Explor.* **2018**, *188*, 95–100. [CrossRef]
58. Afshin, S.; Rashtbari, Y.; Shirmardi, M.; Vosoughi, M.; Hamzehzadeh, A. Adsorption of Basic Violet 16 dye from aqueous solution onto mucilaginous seeds of *Salvia sclarea*: Kinetics and isotherms studies. *Desalin. Water Treat.* **2019**, *161*, 365–375. [CrossRef]
59. Gupta, V.K.; Jain, R.; Shrivastava, M.; Nayak, A. Equilibrium and Thermodynamic Studies on the Adsorption of the Dye Tartrazine onto Waste "Coconut Husks" Carbon and Activated Carbon. *J. Chem. Eng. Data* **2010**, *55*, 5083–5090. [CrossRef]
60. Bryś, A.; Bryś, J.; Ostrowska-Ligęza, E.; Kaleta, A.; Górnicki, K.; Głowacki, S.; Koczoń, P. Wood biomass characterization by DSC or FT-IR spectroscopy. *J. Therm. Anal. Calorim.* **2016**, *126*, 27–35. [CrossRef]
61. Chen, X.; Liu, L.; Luo, Z.; Shen, J.; Ni, Q.; Yao, J. Facile preparation of a cellulose-based bioadsorbent modified by hPEI in heterogeneous system for high-efficiency removal of multiple types of dyes. *React. Funct. Polym.* **2018**, *125*, 77–83. [CrossRef]
62. Ranjbari, S.; Ayati, A.; Tanhaei, B.; Al-Othman, A.; Karimi, F. The surfactant-ionic liquid bi-functionalization of chitosan beads for their adsorption performance improvement toward Tartrazine. *Environ. Res.* **2022**, *204*, 111961. [CrossRef] [PubMed]
63. Goscianska, J.; Ciesielczyk, F. Lanthanum enriched aminosilane-grafted mesoporous carbon material for efficient adsorption of tartrazine azo dye. *Microporous Mesoporous Mater.* **2019**, *280*, 7–19. [CrossRef]
64. Zhang, Q.; Zhang, P.; Pei, Z.; Wang, D. Investigation on characteristics of corn stover and sorghum stalk processed by ultrasonic vibration-assisted pelleting. *Renew. Energy* **2017**, *101*, 1075–1086. [CrossRef]
65. Al-Lagtah, N.M.A.; Al-Muhtaseb, A.H.; Ahmad, M.N.M.; Salameh, Y. Chemical and physical characteristics of optimal synthesised activated carbons from grass-derived sulfonated lignin versus commercial activated carbons. *Microporous Mesoporous Mater.* **2016**, *225*, 504–514. [CrossRef]
66. Wang, H.; Wang, S.; Gao, Y. Cetyl trimethyl ammonium bromide modified magnetic biochar from pine nut shells for efficient removal of acid chrome blue K. *Bioresour. Technol.* **2020**, *312*, 123564. [CrossRef] [PubMed]
67. Rinaldi, R.; Yasdi, Y.; Hutagalung, W.L.C. Removal of Ni (II) and Cu (II) ions from aqueous solution using rambutan fruit peels (*Nephelium lappaceum* L.) as adsorbent. *AIP Conf. Proc.* **2018**, *2026*, 020098. [CrossRef]
68. Zhuang, J.; Li, M.; Pu, Y.; Ragauskas, A.J.; Yoo, C.G. Observation of Potential Contaminants in Processed Biomass Using Fourier Transform Infrared Spectroscopy. *Appl. Sci.* **2020**, *10*, 4345. [CrossRef]
69. Hospodarova, V.; Singovszka, E.; Stevulova, N. Characterization of Cellulosic Fibers by FTIR Spectroscopy for Their Further Implementation to Building Materials. *Am. J. Anal. Chem.* **2018**, *9*, 303–310. [CrossRef]
70. Villabona-ortíz, Á.; Tejada-tovar, C.; Ortega-Toro, R.; Aguilar-Bermúdez, F.; Pájaro-Moreno, Y. Synthesis of adsorbents from wheat hulls, extracted cellulose and modified with Cetyl trimethyl ammonium chloride to remove Congo Red in aqueous solution. *Rev. Mex. Ing. Química* **2021**, *20*, 1–12. [CrossRef]
71. Banerjee, S.; Chattopadhyaya, M.C. Adsorption characteristics for the removal of a toxic dye, tartrazine from aqueous solutions by a low cost agricultural by-product. *Arab. J. Chem.* **2017**, *10*, S1629–S1638. [CrossRef]
72. Hu, Q.; Chen, N.; Feng, C.; Hu, W.; Liu, H. Kinetic and isotherm studies of nitrate adsorption on granular Fe–Zr–chitosan complex and electrochemical reduction of nitrate from the spent regenerant solution. *RSC Adv.* **2016**, *6*, 61944–61954. [CrossRef]
73. Shen, Z.; Zhang, Y.; McMillan, O.; Jin, F.; Al-Tabbaa, A. Characteristics and mechanisms of nickel adsorption on biochars produced from wheat straw pellets and rice husk. *Environ. Sci. Pollut. Res.* **2017**, *24*, 12809–12819. [CrossRef] [PubMed]
74. Silva, F.C.; Lima, L.C.B.; Bezerra, R.D.S.; Osajima, J.A.; Filho, E.C.S. Use of Cellulosic Materials as Dye Adsorbents—A Prospective Study. In *Cellulose—Fundamental Aspects and Current Trends*; InTech: London, UK, 2015; pp. 115–132.

75. Saha, N.; Saba, A.; Reza, M.T. Effect of hydrothermal carbonization temperature on pH, dissociation constants, and acidic functional groups on hydrochar from cellulose and wood. *J. Anal. Appl. Pyrolysis* **2019**, *137*, 138–145. [CrossRef]
76. Gautam, R.K.; Gautam, P.K.; Banerjee, S.; Rawat, V.; Soni, S.; Sharma, S.K.; Chattopadhyaya, M.C. Removal of tartrazine by activated carbon biosorbents of *Lantana camara*: Kinetics, equilibrium modeling and spectroscopic analysis. *J. Environ. Chem. Eng.* **2015**, *3*, 79–88. [CrossRef]
77. Dawood, S.; Sen, T.K.; Phan, C. Synthesis and characterisation of novel-activated carbon from waste biomass pine cone and its application in the removal of congo red dye from aqueous solution by adsorption. *Water. Air. Soil Pollut.* **2014**, *225*, 1818. [CrossRef]
78. Mushtaq, M.; Bhatti, H.N.; Iqbal, M.; Noreen, S. Eriobotrya japonica seed biocomposite efficiency for copper adsorption: Isotherms, kinetics, thermodynamic and desorption studies. *J. Environ. Manag.* **2016**, *176*, 21–33. [CrossRef] [PubMed]
79. Dawodu, M.O.; Akpomie, K.G. Evaluating the potential of a Nigerian soil as an adsorbent for tartrazine dye: Isotherm, kinetic and thermodynamic studies. *Alexandria Eng. J.* **2016**, *55*, 3211–3218. [CrossRef]
80. Reck, I.M.; Paixão, R.M.; Bergamasco, R.; Vieira, M.F.; Vieira, A.M.S. Removal of tartrazine from aqueous solutions using adsorbents based on activated carbon and *Moringa oleifera* seeds. *J. Clean. Prod.* **2018**, *171*, 85–97. [CrossRef]
81. Zhang, J.; Zhang, P.; Zhang, S.; Zhou, Q. Comparative Study on the Adsorption of Tartrazine and Indigo Carmine onto Maize Cob Carbon. *Sep. Sci. Technol.* **2014**, *49*, 877–886. [CrossRef]